Available online at www.sciencedirect.com
SCIENCE DIRECT
Tetrahedron: Asymmetry
Tetrahedron: *Asymmetry* 17 (2006) 822–828

Influence of Lewis acids on the [4+2] cycloaddition of (2*R*,2′*R*)-*N*,*N*′-fumaroylbis[fenchane-8,2-sultam] to cyclopentadiene and cyclohexadiene

Agnieszka Chojnacka,[a] Anna M. Piątek,[a] Christian Chapuis[b,*,†] and Janusz Jurczak[a,b,*]

[a]*Department of Chemistry, University of Warsaw, Pasteura 1, PL-02-093 Warsaw, Poland*
[b]*Institute of Organic Chemistry, Polish Academy of Sciences, Kasprzaka 44/52, PL-01-224 Warsaw, Poland*

Received 20 January 2006; accepted 30 January 2006

Abstract—Compared to the analogous bornane-10,2-sultam derived dienophile (−)-**1b**, the reversed topology observed during the [4+2] cycloaddition of cyclopentadiene or cyclohexadiene to the (−)-**1a**–$TiCl_4$ chelate can be rationalised on the basis of IR studies of their complexes with different Lewis acids. According to X-ray analyses, the origin of this differentiation resides in the loss of masked C_2 symmetry, due to the pseudoequatorial 'down' orientation of the S=O(1) bond in (−)-**1a**,**c** as compared to the pseudo-equatorial 'up' direction adopted by the S=O(2) bond in (−)-**1b**,**d**, associated with the steric influence of the apical Ti–Cl atoms. Dependent on the strength of the Lewis acid, the much higher constraint of the SO_2/C=O *syn-s*-cis conformer diminishes the chelating properties of this type of fenchane-8,2-sultam derived dienophiles (−)-**1a** and **1c**.

1. Introduction

Recently, we reported the preparation of dienophile (−)-**1a** as well as its cycloaddition to cyclopentadiene **2a**.[1] The fenchane derived dienophile (−)-**1a** proved to be slightly less reactive than its camphor sultam analogue (−)-**1b**.[2] Nevertheless, the uncatalysed reaction in CH_2Cl_2 at −78 °C occurs smoothly to afford the major cycloadduct (2*R*,3*R*)-**3a** in 92% conversion and 82% de.[1] Both diastereoisomers of **3a** were obtained pure by CC on SiO_2 and the absolute configuration of the main diastereoisomer ascertained by chiroptical analysis of the known corresponding diol (2*R*,3*R*)-**4a**.[3] In contrast to (−)-**1b**, we were surprised to observe a reverse sense of induction when the reaction was mediated at −78 °C by 1.0 mol equiv of $TiCl_4$ in CH_2Cl_2 (>99% conversion, 20% de). Herein, we report in more detail the influence of the *Lewis* acid on this cycloaddition (Scheme 1).

2. Results and discussion

The screening began by varying quantities of $TiCl_4$, as reported in Table 1 (entries 1–5). Both conversion and ratio of the main diastereoisomer (2*S*,3*S*)-**3a** were determined by ^1H NMR analysis of the cycloadduct.[1] The selectivity rose from 9% to 27% de by increasing the amount of $TiCl_4$ from 0.25 to 1.5 mol equiv, while the conversion decreased from 98% to 34% when an excess of $TiCl_4$ was used. This suggests that double chelation either sterically diminishes access to the dienophile or favours a less reactive conformation. At this point we also wondered about the stability of the cycloadduct and consequently treated pure (2*R*,3*R*)-**3a** with 1.00 mol equiv of $TiCl_4$ for 24 h at −78 °C in CH_2Cl_2, but noticed no modification or alteration. This experiment was then repeated in the presence of an excess amount of diene **2a**, without diminution of the purity. We can thus exclude any problem of chemical stability or thermodynamic equilibration either via selective polymerisation or retro Diels–Alder reaction, as proposed earlier for another heterodienophile of this type.[4,5] The preferred formation of the (2*S*,3*S*)-stereoisomer **3a** seems specific to $TiCl_4$, since with other Lewis acids, the more selective reverse topology was preferred.

* Corresponding authors. E-mail addresses: Christian.chapuis@firmenich.com; jjurczak@chem.uw.edu.pl
† Present address: Firmenich SA, Corporate R&D Division, PO Box 239, CH-1211 Geneva 8, Switzerland.

0957-4166/$ - see front matter © 2006 Elsevier Ltd. All rights reserved.
doi:10.1016/j.tetasy.2006.01.031

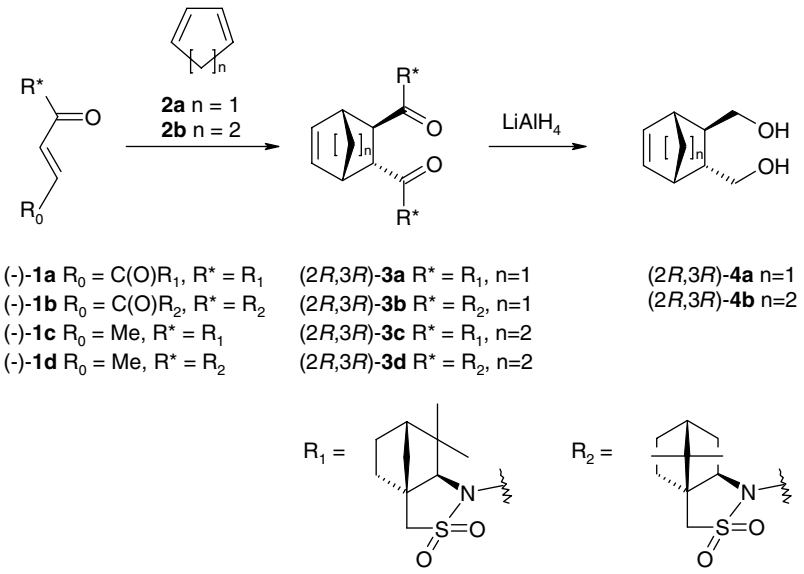

Scheme 1.

Table 1. Cycloaddition of (−)-**1a** to cyclopenta-1,3-diene **2a** in CH_2Cl_2 at −78 °C for 24 h in the presence of a Lewis acid

Entry	Lewis acid	Amount	Conversion (%)	de (%)
1	$TiCl_4$	0.25	98	−9
2	$TiCl_4$	0.50	98	−11
3	$TiCl_4$	1.00	99	−20
4	$TiCl_4$	1.50	73	−27
5	$TiCl_4$	2.5	34	−25
6	$TiCl_3$(O*i*-Pr)	1.00	97	87
7	$TiCl_2$(O*i*-Pr)$_2$	1.00	99	89
8	TiCl(O*i*-Pr)$_3$	1.00	61	82
9	Ti(O*i*-Pr)$_4$	1.00	58	80
10	$ZrCl_4$	1.00	98	87
11	$SnCl_4$	1.00	57	99
12	$SnCl_4$	1.00	99[a]	99
13	$AlCl_3$	1.00	98	89
14	$AlCl_2Me$	1.00	93	83
15	$AlCl_2Et$	1.00	90	88
16	$AlClMe_2$	1.00	99	99
17	$AlClEt_2$	1.00	27	88
18	$AlMe_3$	1.00	99	35
19	$AlEt_3$	1.00	31	80
20	$ZnBr_2$[b]	1.00	19	83
21	$BF_3{\cdot}OEt_2$	1.00	7	(2*R*,3*R*)-**3a**[c]

[a] 48 h.
[b] No conversion was observed with $ZnCl_2$.
[c] Quantitative determination outside the precision range (±2%).

Indeed, when one or two isopropoxide units replaced the Cl atoms in $TiCl_4$, practically full conversion and 87–89% de were attained in favour of diastereoisomer (2*R*,3*R*)-**3a**, while replacement with three or four isopropoxide ligands resulted in both poorer conversions (58–61%) and diastereoselectivities (80–82%). These latter results are close to those reported recently under uncatalysed conditions.[1] The analogous Lewis acid $ZrCl_4$ behaves,[6] in contrast to $TiCl_4$, similarly to $TiCl_3$(O*i*-Pr), with 98% conversion and 87% de. We were pleased to reach full selectivity with $SnCl_4$, albeit with only 57% conversion. This drawback was overcome by waiting 48 h to reach full conversion (entry 12). Several Lewis acids derived from alkyl aluminiums[7] were also tested and compared to $AlCl_3$ (entry 13, 98% conversion, 89% de). Me_2AlCl was by far the most efficient in this series (entry 16), although we generally observed both better stereoselectivities and lower conversions with the sterically more demanding Et, as compared to Me substituents, in contrast to the analogous dienophile (−)-**1b**.[8] Finally, both $ZnBr_2$ and the nonchelating $BF_3{\cdot}OEt_2$ gave a very poor conversion for the (2*R*,3*R*) cycloadduct **3a**. In order to gain some more insight on the unique and specific role of $TiCl_4$, we performed comparative IR analyses[9] of the free, as well as 1:1 $TiCl_4$[7] and $SnCl_4$ complexes of (−)-**1a**,**b**, as well as the more simple *N*-crotonoyl sultams (−)-**1c**,**d**, whose free[1,7] or chelated[10] conformations in the solid state, based on their X-ray structure analyses, were earlier reported. These results are summarised in Table 2.

The significant modifications as indicated in bold concern both the magnitude of the bathochromic/hypochromic shifts of the νC═O from 1674–1683 to 1532–1654 cm^{-1} for this chelated/coordinated functionality, as well as the hypsochromic shift of the asymmetric SO_2 stretching from 1332–1347 to 1392–1412 cm^{-1}, while the symmetric νSO_2 around 1135–1149 cm^{-1} is less affected. If we focus on the conformationally and functionally more simple *N*-crotonoyl sultams (−)-**1c** and **1d**, we can see that coordination with $TiCl_4$ leads to a red shift from 1682–1683 to 1532–1528 cm^{-1}, respectively. Furthermore, in the presence of $TiCl_4$, the C═O stretching at 1683 cm^{-1} totally disappears for the camphor sultam derivative (−)-**1d**, while a weak residual signal at 1682 cm^{-1} remains visible for the coordinated fenchane analogue (−)-**1c**, thus displaying weaker chelating properties for this latter skeleton, due to a higher conformational constraint.[1] This propensity is even more accentuated with the weaker $SnCl_4$ complex, since in the case of the fenchane derived sultam (−)-**1c**, the red shift is less pronounced at 1559 cm^{-1}

Table 2. IR analyses of (−)-**1a–d** and their 1:1 $TiCl_4$ or $SnCl_4$ complexes in CH_2Cl_2 (cm^{-1})

(−)-**1a**	(−)-**1a**–$TiCl_4$	(−)-**1a**–$SnCl_4$	(−)-**1b**	(−)-**1b**–$TiCl_4$	(−)-**1b**–$SnCl_4$	(−)-**1c**	(−)-**1c**–$TiCl_4$	(−)-**1c**–$SnCl_4$	(−)-**1d**	(−)-**1d**–$TiCl_4$	(−)-**1d**–$SnCl_4$	
2976m	2971m	2976m	2965m	2967m	2965m	2977m	2973m	2976m	2964s	2969m	2966s	νC–H
1674s	1681w	1674m	1676s	1679m	1676s	1682s	1682w	1682m	1683s		1683s	νC=O
1634w	1637w	1627m	1639w	1639w	1640w	1641s	1640s	1642m	1642s	1638s	1642s	νC=C
	1563s	**1654m**		**1560s**			**1532s**	**1559w**		**1528s**	**1528s**	νC=O···
1452w	1453w	1452w	1457w	1459w	1457w	1445w	1440m	1444m	1444m	1440m	1443m	CH_2
	1404s			**1413s**			**1396s**	**1411w**		**1410m**	**1412m**	ν_aSO_2···
1370m		1370m	1375m		1375m	1366w		1368m	1374m			Me_2C
										1349s		
1341s	1347s	1336s	1340s	1346s	1340s	1336s	1338s	1337s	1332s	1338s	1336s	ν_aSO_2
1324s	1317m		1321s	1316m	1321s	1296m	1317m	1296m	1300m	1305w	1305w	
1214s	1220m	1215m	1210s	1214m	1210s	1227m	1232m	1218m	1216s	1224w	1216s	
1169s	1175m	1170m	1166m	1167m	1167m	1171m	1175m	1172m	1166m		1168m	C–N
1149s	1144m	1149m	1137s	1138m	1137s	1146m	1145m	1147m	1135m	1135w	1135m	ν_sSO_2
							1107m			**1115m**		ν_sSO_2···
1109w	1106m	1109w	1118w	1117m	1118w	1124w	1122m	1125w	1105w	1100w	1112w	CH_3
1086m	1085w	1086m	1069m	1068w	1069m	1083m	1084w	1083m	1066m		1066m	CH_2
1045m	1032w	1043w	1046w		1046w	1044m	1044w	1044m	1048m	1047w	1048w	C–C

while the residual signal at 1682 cm^{-1} is more intense. The asymmetric SO_2 stretch of the fenchane sultam derived dienophile (−)-**1c** is much more affected by $TiCl_4$, with the apparition of an intense signal at 1396 cm^{-1}, in contrast to the weak band at 1411 cm^{-1} observed for its $SnCl_4$ complex. Similar properties were noticed for the *N*,*N*′-fumaroyl sultams (−)-**1a** and **1b**. Indeed, the red νC=O shift is much more pronounced with $TiCl_4$ (1563 cm^{-1}) than with $SnCl_4$ (1654 cm^{-1}), while the intensity of the residual signal at 1637 cm^{-1} is much weaker for $TiCl_4$. Additionally, the asymmetric SO_2 stretching is also much more affected, as shown by the apparition of a strong signal at 1404 cm^{-1} in the case of the (−)-**1a**–$TiCl_4$ chelate, as compared to either the (−)-**1a**–$SnCl_4$ or (−)-**1b**–$SnCl_4$ complex, which even seems unaffected in this latter case. The symmetric νSO_2 is slightly modified, but only in the case of $TiCl_4$ chelation with (−)-**1c** and **1d**, with the apparition of a signal at 1107 and 1115 cm^{-1}, respectively. These facts suggest that the $TiCl_4/SnCl_4$ chelation of (−)-**1c** is less favoured than (−)-**1d** due to the presence of the C(3)Me_2 substitution, and that $TiCl_4$ chelates well with (−)-**1a** and **1b**, while weaker Lewis acids, such as $SnCl_4$, seem only to coordinate with their C=O moiety(ies), eventually by intermolecular bis-complexation.

Based on both these comparative IR analyses and the X-ray structure analyses of (−)-**1c** and **1d**, we suggest the following hypothesis to rationalise the observed stereochemical course of this cycloaddition. The X-ray analyses of (−)-**1c** and **1d**[1,7] exhibit, in both cases, a thermodynamically more stable *anti* SO_2/C(O) *s*-cis C=O/C=C conformation. In both cases, the N atom is pyramidalised in the same direction, but the absence of the C(7) *gem*-dimethyl substitution in (−)-**1c** allows its S=O(2) bond to adopt a pseudoaxial orientation, in contrast to (−)-**1d**, which projects its S=O(1) substituent in the opposite pseudoaxial direction. This fact has two consequences on the directing effect of these chiral auxiliaries. Firstly, (−)-**1d** possesses a masked C_2 symmetry, as suggested by Curran et al.,[11] invariably directing the attack on the Cα-*re* face, whichever SO_2/C(O) *syn*- or *anti*-*s*-cis conformation is adopted, opposite either to the C(2)–C(3) or the axial S=O(1) substituents, respectively. The second point is that the 'up' pseudoequatorial orientation of the S=O(2) bond in the chelated (−)-**1d**–$TiCl_4$ complex[10] directs one of the apical Ti–Cl substituents towards the C(7) atom, thus sterically reinforcing the π-facial shielding of both the Me(8) and C(3) atoms and favouring an attack on the Cα-*re* face. In contrast, in view of the fact that complexation with the pseudoaxial S=O(2) substituent is energetically unfavourable,[1] the (−)-**1c**–$TiCl_4$ chelate, with its 'down' pseudoequatorial S=O(1) bond, orientates both the bottom apical Ti–Cl atom and the Me(9) on the opposite face to the C(3)–Me(8) moiety. As a consequence, both π-faces are sterically hindered and could possibly explain the poor and reverse selectivity, as well as the lower reactivity of (−)-**1a** as a bis-chelated entity in the presence of an excess of $TiCl_4$. In the case of a weaker or nonchelating Lewis acid, coordination to the more basic *anti* C=O lone pair, *anti*-periplanar to the (O)C–Cα bond, is sterically excluded by the

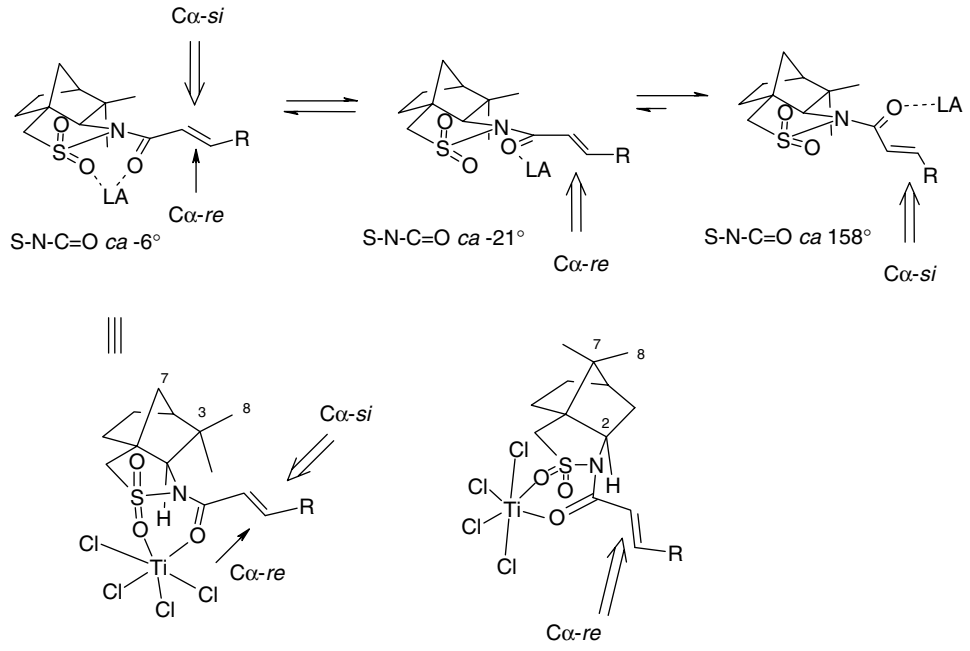

Scheme 2. Reactive chelated or coordinated conformations with, for clarity, arbitrary numbering of the fenchane skeleton.

C(3)–Me_2 substituents of (−)-**1a** and **1c**. In such a case, as for the uncatalysed conditions, the *syn-s*-cis O=S=O bisecting conformation, with a larger S–N–C=O dihedral angle than the chelate itself,[1] could eventually be more reactive than the thermodynamically more stable *anti-s*-cis conformer, thus explaining the beneficial statistical effect of a higher temperature (Scheme 2).[1]

With these tentative rationalisations in mind, we then extended the scope of the cycloaddition of (−)-**1a** to cyclohexadiene **2b**. Due to the lower reactivities of both partners, it was necessary to adjust the reaction temperature to 0 °C, in order to observe appreciable conversions in CH_2Cl_2. Under these conditions, 1.0 mol equiv of $ZrCl_4$ afforded the main cycloadduct (−)-(2*R*,3*R*)-**3c** with 56% conversion after 24 h or 74% conversion after 72 h and 82% de. Absolute configuration was based on an X-ray structure analysis of the CC purified and then crystallised material, rather than on the chiroptical properties of the diol (2*R*,3*R*)-**4b**,[12] while the diastereoselectivity and conversion were measured directly on the cycloadduct by integration in the ^{1}H NMR spectrum of the olefinic protons at 6.09 and 6.52 ppm, by analogy with (−)-(2*R*,3*R*)-**3d**.[8] The minor (2*S*,3*S*) stereoisomer **3c** exhibits the corresponding signals at 6.20 and 6.52 ppm. This latter isomer was also obtained as the main diastereoisomer (98% conversion, 17% de) when the cycloaddition at 0 °C in CH_2Cl_2 was performed in the presence of 1.0 mol equiv of $TiCl_4$ for 72 h.

The structural analysis of cycloadduct (−)-(2*R*,3*R*)-**3c** is noteworthy. Although pyramidalised in the same manner, the N atoms are even more planar than in the case of (−)-**1c** (0.155(2) [Å][1]) due to the strong steric requirement of the bicyclic [2.2.2] system, as expressed by either their Δ*h*N values (see Table 3) or the sum of their substituent angles[13] (357.55° and 358.55° as compared to 356.86°[1]). Both sultam units show typical SO_2/C=O anti-conformations,[14] resulting from dipole/dipole repulsions,[10] while the S=O(2) substituents are even more pseudoaxial than in the case of (−)-**1c** (−101.73(12)° and −95.27(12)° as compared to −105.50(16)°[1] for the C(2)–N–S=O(2) torsional angle). This is also shown by the smaller five-membered ring puckering parameters ϕ_2 of 132.1° and 139.7°, as opposed to 299.0° for the camphor derived *N*-crotonoyl sultam (−)-**1d**,[1] which directs its S=O(2) substituent in the pseudoequatorial direction.

3. Conclusion

Displacement of the *gem*-dimethyl moiety from the C(7) to the C(3) position in (−)-**1d** and **1c** results in at least two main differences. Firstly, with respect to the thermodynamically more stable *anti-s*-cis conformation, the SO_2/C=O *syn-s*-cis conformer is four times higher in energy for (−)-**1c** as compared to (−)-**1d**.[1] Secondly, the S=O(1) substituent is orientated in the pseudoequatorial direction for (−)-**1c**, while this position is occupied by the S=O(2) moiety in the case of (−)-**1d**. Besides the loss of masked C_2 symmetry, these features imply that chelation of (−)-**1c** is effective only with a strong chelating Lewis acid, such as $TiCl_4$, while simple coordination to the carbonyl group occurs in the presence of weaker Lewis acids. As a result, the bottom apical Cl atom of the chelated (−)-**1c**–$TiCl_4$ complex is responsible for the consequential Cα-*re* π-face shielding, while the top apical Cl atom participates in the Cα-*si* π-face shielding for the (−)-**1d**–$TiCl_4$ chelate.

The synthesis, as well as comparative structural, conformational and inductive properties of sultam analogues lacking geminal Me groups at both C(3) and C(7) are

Table 3. Selected bond lengths [Å] and angles [°] for (−)-(2*R*,3*R*)-**3c**

S=O(1)	1.4296(13)	S′=O(1′)	1.4273(13)
S=O(2)	1.4333(12)	S′=O(2′)	1.4354(12)
S–N	1.6907(13)	S′–N′	1.6890(13)
S–C(10)	1.7725(18)	S′–C(10′)	1.7682(17)
N–C(2)	1.487(2)	N′–C(2′)	1.4865(19)
N–C(11)	1.406(2)	N′–C(11′)	1.4133(19)
O(3)=C(11)	1.2113(19)	O(3′)=C(11′)	1.2118(19)
C(11)–C(12)	1.513(2)	C(11′)–C(12′)	1.500(2)
C(12)–C(12′)	1.538(2)	C(15)–C(15′)	1.479(3)
C(14)–C(14′)	1.384(3)	C(12′)–C(13′)	1.569(2)
O(1)=S=O(2)	117.67(8)	O(1′)=S′=O(2′)	117.19(8)
C(2)–N–S	112.69(10)	C(2′)–N′–S′	112.58(10)
C(2)–N–C(11)	119.44(13)	C(2′)–N′–C(11′)	119.15(13)
S–N–C(11)	125.42(11)	S′–N′–C(11′)	126.82(11)
O(3)=C(11)–N	118.39(15)	O(3′)=C(11′)–N′	117.88(14)
N–C(11)–C(12)	117.10(14)	N′–C(11′)–C(12′)	117.37(14)
O(3)=C(11)–C(12)	124.22(15)	O(3′)=C(11′)–C(12′)	124.70(14)
C(2)–N–S=O(1)	127.27(12)	C(2′)–N′–S′=O(1′)	133.95(12)
C(2)–N–S=O(2)	−101.73(12)	C(2′)–N′–S′=O(2′)	−95.27(12)
C(3)–C(2)–N–S	126.05(13)	C(3′)–C(2′)–N′–S′	120.76(13)
C(11)–N–S=O(1)	−34.72(15)	C(11′)–N′–S′=O(1′)	−32.02(16)
O(3)–C(11)–C(12)–C(12′)	168.26(13)	O(3′)–C(11′)–C(12′)–C(12)	169.31(14)
S–N–C(11)=O(3)	161.10(12)	S′–N′–C(11′)=O(3′)	169.68(12)
Δ*h*N	0.138(2)	Δ*h*N′	0.106(2)
Puckering parameters q_2	0.381	Puckering parameters q_2	0.402
S–N–C(2)–C(1)–C(10) ϕ_2	132.1	S′–N′–C(2′)–C(1′)–C(10′) ϕ_2	139.7

currently being studied in our laboratories. These results should help us to determine if the pseudoaxial orientation of the S=O(2) in (−)-**1c** is due either to the absence of the C(7)–Me(8) substituent or to the steric influence of the Cα–H moiety, and whether or not an identical tilting of the N atom is maintained.[15]

4. Experimental

General, see Ref. 16. All measurements of crystals were performed on a KM4CCD κ-axis diffractometer with graphite-monochromated Mo K_α radiation. The crystal was positioned at 62 mm from the CCD camera. One thousand and six hundred frames were measured at 0.75° intervals with a counting time of 18 s. The data were corrected for *Lorentz* and polarisation effects. Empirical correction for absorption was applied.[17] Data reduction and analysis were carried out with the Oxford Diffraction programs.[18] The structure was solved by direct methods[19] and refined using SHELXL.[20] The refinement was based on F^2 for all reflections except those with very negative F^2. Weighted R factors wR and all goodness-of-fit S values are based on F^2. Conventional R factors are based on F with F set to zero for negative F^2. The $F_o^2 > 2\sigma(F_o^2)$ criterion was used only for calculating R factors and is not relevant to the choice of reflections for the refinement. The R factors based on F^2 are about twice as large as those based on F. All hydrogen atoms were located geometrically and positions and temperature factors of most of them were refined. Scattering factors were taken from Tables 6.1.1.4 and 4.2.4.2 of Ref. 21. The known configurations of the asymmetric centres were confirmed by the Flack-parameter refinement.[22] The Cremer and Pople puckering parameters[23] were calculated according to the literature (Table 4).[24] Crystallographic data (excluding structural factors) for structure (−)-(2*R*,3*R*)-**3c** (Fig. 1) has been deposited as supplementary material

Table 4. Crystal data and structure refinement of compounds (−)-(2*R*,3*R*)-**3c**

Empirical formula	$C_{30}H_{42}N_2O_6S_2$
Molecular weight	590.78
Temperature (K)	100(2)
Wavelength (Å)	0.71073
Crystal system	Monoclinic
Space group	$P2_1$
Unit-cell dim.	
a [Å]	6.7060(5), $\alpha = 90.0°$
b [Å]	17.3160(11), $\beta = 104.376(6)°$
c [Å]	12.7582(9), $\gamma = 90.0°$
Volume [Å^3]	1435.11(17)
Z	2
Density [Mg/m^3]	1.367
Absorpt. coeff. [mm^{-1}]	0.233
$F(000)$ Electrons	632
Crystal size [mm]	$0.30 \times 0.17 \times 0.12$
θ Range for data [°]	2.87–28.80
Index ranges	$-9 \leqslant h \leqslant 8$
	$-23 \leqslant k \leqslant 23$
	$-17 \leqslant l \leqslant 17$
Reflections collected	27514/6984
R(int)	0.0319
Refinement method	Full-matrix least-squares on F^2
Data/restraints/parameters	6984/1/518
Goodness-of-fit on F^2	0.872
$R(F)$ [$I > 2\sigma(I)$]	0.0295
$wR(F^2)$ (all data)	0.0513
Abs. struct. parameter	−0.04(4)
Extinction coefficient	0.0045(4)
Largest peak and holes [e Å^{-3}]	0.271, −0.266

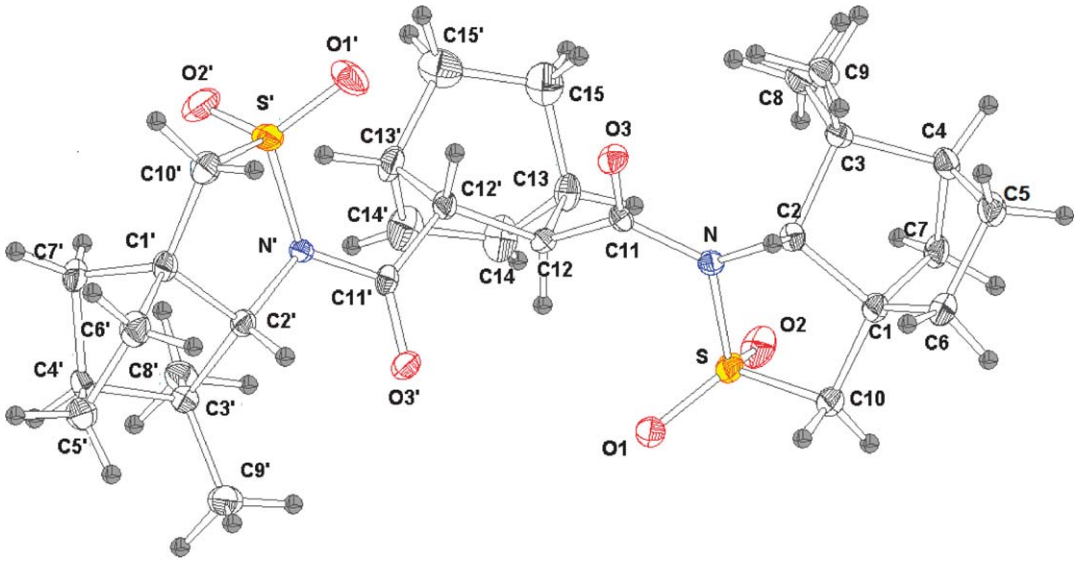

Figure 1. ORTEP representation of (−)-(2*R*,3*R*)-**3c** with arbitrary atom numbering. Ellipsoids are represented at the 50% probability level.

with the Cambridge Crystallographic Data Centre and allocated the deposition number CCDC 294630. Copies of the data can be obtained free of charge on application to CCDC, 12 Union Road, Cambridge CB2 1EW, UK (fax: int. code + (1223)336-033; e-mail: deposit@ccdc.cam.ac.uk).

4.1. (2*R*,3*R*)-Bicyclo[2.2.1]hept-5-ene-2,3-diyl]bis[(3a*S*,6*S*,7a*R*)-1,4,5,6,7,7a-hexahydro-7,7-dimethyl-2,2-dioxido-3*H*-3a,6-methano-2,1-benzothiazol-1-yl]methanone] (−)-(2*R*,3*R*)-3a

The appropriate Lewis acid (1 M in CH_2Cl_2, 100 μl, 0.1 mmol) was added to a soln of (−)-**1a** (51 mg, 0.1 mmol) in CH_2Cl_2 (2 ml), then the mixture was cooled to −78 °C and cyclopentadiene (83 μl, 1.0 mmol) was added slowly along the wall of the flask. After 24 h at −78 °C, the reaction mixture was quenched with NH_4F and warmed to 20 °C. After the addition of H_2O, the mixture was extracted with CH_2Cl_2. The organic phase was dried over $MgSO_4$ and concentrated. Both conversion and de were measured by integration of the olefinic protons by means of ^{1}H NMR analysis. A pure oily material was obtained after purification by CC (SiO_2, from toluene to toluene/AcOEt 95:5). For full analyses see Ref. 1.

4.2. (2*R*,3*R*)-Bicyclo[2.2.2]oct-5-ene-2,3-diyl]bis[(3a*S*,6*S*,7a*R*)-1,4,5,6,7,7a-hexahydro-7,7-dimethyl-2,2-dioxido-3*H*-3a,6-methano-2,1-benzothiazol-1-yl]methanone] (−)-(2*R*,3*R*)-3c

A soln of (−)-**1a** (51 mg, 0.1 mmol) in CH_2Cl_2 (2 ml) was added to $ZrCl_4$ (23.3 mg, 0.1 mmol) at 0 °C, after which cyclohexadiene (95 μl, 1.0 mmol) was added dropwise. After 72 h at 0 °C, the reaction mixture was quenched with NH_4F and equilibrated to 20 °C. After the addition of H_2O, the mixture was extracted with CH_2Cl_2. The organic phase was dried over $MgSO_4$ and concentrated. Both conversion (74%) and de (82%) were measured by integration of the olefinic protons by means of ^{1}H NMR analysis. Pure crystalline material was obtained after purification by CC (SiO_2, with hexane/AcOEt 9:1–7:3) in 60% yield. $R_f = 0.4$ hexane/AcOEt 6:4. Mp: 280–290 °C (decomposition). $[\alpha]_D^{20} = -88.7$ (*c* 0.5, $CHCl_3$). IR: 2951, 2875, 1692, 1633, 1330, 1221, 1166, 1146, 1123, 1085, 1044, 1026, 545. ^{1}H NMR: 0.89 (s, 3H), 0.92 (s, 3H), 1.20 (s, 3H), 1.26 (s, 3H), 1.3–1.9 (m, 16H), 2.43 (d, $J = 10$, 2H), 3.10 (br s, 1H), 3.18 (br s, 1H), 3.35 (d, $J = 13$, 2H), 3.44 (dd, $J = 13$, 5, 2H), 3.54 (s, 1H), 3.62 (s, 1H), 4.13 (br s, 1H), 4.22 (d, $J = 5$, 1H), 6.09 (t, $J = 7.5$, 1H), 6.53 (t, $J = 7.5$, 1H). ^{13}C NMR: 19.25 (t), 22.6 (q), 22.9 (q), 23.7 (2t), 25.0 (q), 25.1 (q), 25.9 (t), 32.2 (t), 32.45 (t), 33.55 (d), 34.8 (d), 39.4 (2t), 45.0 (s), 45.1 (s), 45.25 (d), 45.8 (s), 45.9 (s), 46.3 (d), 49.05 (d), 49.1 (d), 54.4 (t), 54.5 (t), 74.1 (d), 74.4 (d), 131.5 (d), 134.9 (d), 173.2 (s), 174.2 (s). IHR-MS calcd for $C_{30}H_{42}N_2O_6NaS_2$ 613.2383, found 613.2364.

4.3. (2*S*,3*S*)-Bicyclo[2.2.2]oct-5-ene-2,3-diyl]bis[(3a*S*,6*S*,7a*R*)-1,4,5,6,7,7a-hexahydro-7,7-dimethyl-2,2-dioxido-3*H*-3a,6-methano-2,1-benzothiazol-1-yl]methanone] (−)-(2*S*,3*S*)-3c

$TiCl_4$ (1 M in CH_2Cl_2, 100 μl, 0.1 mmol) was added to a soln of (−)-**1a** (51 mg, 0.1 mmol) in CH_2Cl_2 (2 ml) after which the mixture was cooled to −78 °C and cyclohexadiene (100 μl, 1.0 mmol) added slowly along the wall of the flask. After 72 h at −78 °C, the reaction mixture was quenched with NH_4F and equilibrated to 20 °C. After addition of H_2O, the mixture was extracted with CH_2Cl_2. The organic phase was dried over $MgSO_4$ and concentrated. Both conversion and de were measured by integration of the olefinic protons by means of ^{1}H NMR analysis. Pure crystalline material was obtained after purification by CC (SiO_2, hexane/AcOEt 9:1–7:3). $R_f = 0.59$ hexane/AcOEt 6:4. $[\alpha]_D^{20} = -4.5$ (*c* 0.6, $CHCl_3$). IR: 2951, 2875, 1692, 1633, 1330, 1221, 1166, 1146, 1123, 1085, 1044, 1026, 545. ^{1}H NMR:

0.85 (s, 3H), 0.92 (s, 3H), 1.24 (s, 3H), 1.31 (s, 3H), 1.2–2.0 (m, 16H), 2.30 (t, $J = 10$, 2H), 3.0 (br s, 1H), 3.07 (br d, $J = 5$, 1H), 3.23 (d, $J = 5.5$, 1H), 3.41 (m, 3H), 3.49 (s, 2H), 3.54 (m, 2H), 6.20 (t, $J = 7$, 1H), 6.54 (t, $J = 7$, 1H). ^{13}C NMR: 17.8 (t), 22.8 (2q), 23.6 (t), 23.7 (t), 25.0 (q), 25.0 (t), 25.1 (q), 32.3 (t), 32.4 (d), 32.45 (t), 33.3 (d), 39.3 (2t), 45.0 (s), 45.1 (s), 45.9 (s), 45.95 (s), 48.0 (d), 49.1 (d), 49.15 (d), 50.9 (d), 54.55 (t), 54.7 (t), 74.6 (d), 74.7 (d), 131.55 (d), 134.8 (d), 172.7 (s), 174.4 (s). IHR-MS: calcd for $C_{30}H_{42}N_2O_6NaS_2$ 613.2383, found 613.2389.

Acknowledgements

The X-ray measurements were effected in the Crystallographic Unit of the Physical Chemistry Lab. at the Chemistry Department of the University of Warsaw.

References

1. Piatek, A. M.; Chojnacka, A.; Chapuis, C.; Jurczak, J. *Helv. Chim. Acta* **2005**, *88*, 2441.
2. Chapuis, C.; Rzepecki, P.; Bauer, T.; Jurczak, J. *Helv. Chim. Acta* **1995**, *78*, 145; Bauer, T.; Chapuis, C.; Kucharska, A.; Rzepecki, P.; Jurczak, J. *Helv. Chim. Acta* **1998**, *81, 324.*
3. Horton, D.; Machinami, T. *J. Chem. Soc., Chem. Commun.* **1981**, 88; Horton, D.; Machinami, T.; Takagi, Y. *Carbohydr. Res.* **1983**, *121*, 135; Takano, S.; Kurotaki, A.; Ogasawara, K. *Synthesis* **1987**, 1075; Saito, S.; Hama, H.; Matsuura, Y.; Okada, K.; Moriwake, T. *Synlett* **1991**, 819; Saito, S.; Narahara, O.; Ishikawa, T.; Asahara, M.; Moriwake, T.; Gawronski, J.; Kazmierczak, F. *J. Org. Chem.* **1993**, *58*, 6292.
4. Chapuis, C.; de Saint Laumer, J.-Y.; Marty, M. *Helv. Chim. Acta* **1997**, *80*, 146.
5. Raczko, J.; Achmatowicz, M.; Kwiatkowski, P.; Chapuis, C.; Urbanczyk-Lipkowska, Z.; Jurczak, J. *Tetrahedron: Asymmetry* **2000**, *11*, 1027.
6. For an earlier use of a TMS protected diol–$ZrCl_4$ chiral catalyst in asymmetric [4+2] cycloadditions, see: Chapuis, C.; Jurczak, J. *Helv. Chim. Acta* **1987**, *70*, 436; For a more recent example, see Kobayashi, O.; Ishigai, H. JP 2002356454 A2, (13 December 2002 to *Koho*); *CA*, **2003**, *138*, 39104.
7. Oppolzer, W.; Chapuis, C.; Bernardinelli, G. *Helv. Chim. Acta* **1984**, *67*, 1397.
8. Bauer, T.; Chapuis, C.; Kucharska, A.; Rzepecki, P.; Jurczak, J. *Helv. Chim. Acta* **1998**, *81*, 324.
9. Hagemann, H.; Dulak, M.; Wesolowski, T. A.; Chapuis, C.; Jurczak, J. *Helv. Chim. Acta* **2004**, *87*, 1748.
10. Oppolzer, W.; Rodriguez, I.; Blagg, J.; Bernardinelli, G. *Helv. Chim. Acta* **1989**, *72*, 123.
11. Kim, B. H.; Curran, D. P. *Tetrahedron* **1993**, *49*, 293.
12. Ito, Y. N.; Ariza, X.; Beck, A. K.; Bohac, A.; Ganter, C.; Gawley, R. E.; Kühnle, F. N. M.; Tuluja, T.; Wang, Y. M.; Seebach, D. *Helv. Chim. Acta* **1994**, *77*, 2071.
13. Andrews, P. R.; Munro, S. L. A.; Sadek, M.; Wong, M. G. *J. Chem. Soc., Perkin Trans. 2* **1988**, 711; So, S. P.; Luh, T. Y. *J. Org. Chem.* **1986**, *51*, 1604; Kay, J.; Glick, M. D.; Raban, M. *J. Am. Chem. Soc.* **1971**, *93*, 5224.
14. For two exceptions, see: Bauer, T.; Chapuis, C.; Kiegiel, J.; Krajewski, J. W.; Piechota, K.; Urbanczyk-Lipkowska, Z.; Jurczak, J. *Helv. Chim. Acta* **1996**, *79*, 1059, as well as registration number CCDC 269445.
15. Preliminary B3LYP/6-31G** calculations suggest that, in the case of *N*-crotonoyl isofenchane-8,2-sultam, the difference of energy between the *syn-s*-cis (S–N–C(11)=O(3) = −11.9°) and more stable *anti-s*-cis (S–N–C(11)=O(3) = 163.2°) conformers is close to that of (−)-**1c** (5.3 kcal/mol), while the S=O(2) adopts a pseudoaxial orientation (C(2)–N–S=O(2) = −107.5°) and the N tilting is similar to (−)-**1c**.
16. Chapuis, C.; Kucharska, A.; Rzepecki, P.; Jurczak, J. *Helv. Chim. Acta* **1998**, *81*, 2314; Achmatowicz, M.; Chapuis, C.; Rzepecki, P.; Jurczak, J. *Helv. Chim. Acta* **1999**, *82*, 182.
17. CrysAlis RED, Oxford Diffraction Ltd, Version 1.171.28cycle2 beta (release 25-10-2005 CrysAlis171.NET) (compiled October 25, 2005, 08:50:05). Empirical absorption correction using spherical harmonics, implemented in SCALE3 ABSPACK scaling algorithm.
18. CrysAlis CCD, Oxford Diffraction Ltd, Version 1.171.28cycle2 beta; CrysAlis RED, Oxford Diffraction Ltd, Version 1.171.28cycle2 beta.
19. Sheldrick, G. M. *Acta Crystallogr.* **1990**, *A46*, 467.
20. Sheldrick, G. M. SHELXL93. *Program for the Refinement of Crystal Structures.,* Univ. of Göttingen, Germany.
21. *International Tables for Crystallography*; Wilson, A. J. C., Ed.; Kluwer: Dordrecht, 1992; Vol. C.
22. Flack, H. D. *Acta Crystallogr. Sect. C* **1983**, *39*, 876; Flack, H. D.; Bernardinelli, G. *Acta Crystallogr. Sect. A* **1999**, *55*, 908; Flack, H. D.; Bernardinelli, G. *J. Appl. Crystallogr.* **2000**, *33*, 1143.
23. Cremer, D.; Pople, J. A. *J. Am. Chem. Soc.* **1975**, *97*, 1354.
24. www.hyper.com/support/download/Macros/macros_index.html.